



Modulation of Hematopoietic Injury by a Promising Radioprotector, Gamma-Tocotrienol, in Rhesus Macaques Exposed to Partial-Body Radiation

Authors: Garg, Tarun K., Garg, Sarita, Miousse, Isabelle R., Wise, Stephen Y., Carpenter, Alana D., et al.

Source: Radiation Research, 201(1) : 55-70

Published By: Radiation Research Society

URL: <https://doi.org/10.1667/RADE-23-00075.2>

BioOne Complete (complete.BioOne.org) is a full-text database of 200 subscribed and open-access titles in the biological, ecological, and environmental sciences published by nonprofit societies, associations, museums, institutions, and presses.

Your use of this PDF, the BioOne Complete website, and all posted and associated content indicates your acceptance of BioOne's Terms of Use, available at www.bioone.org/terms-of-use.

Usage of BioOne Complete content is strictly limited to personal, educational, and non - commercial use. Commercial inquiries or rights and permissions requests should be directed to the individual publisher as copyright holder.

BioOne sees sustainable scholarly publishing as an inherently collaborative enterprise connecting authors, nonprofit publishers, academic institutions, research libraries, and research funders in the common goal of maximizing access to critical research.

Modulation of Hematopoietic Injury by a Promising Radioprotector, Gamma-Tocotrienol, in Rhesus Macaques Exposed to Partial-Body Radiation

Tarun K. Garg,^{a,1} Sarita Garg,^{b,c,1} Isabelle R. Miousse,^c Stephen Y. Wise,^{d,e} Alana D. Carpenter,^{d,e}
Oluseyi O. Fatanmi,^{d,e} Frits van Rhee,^a Vijay K. Singh,^{d,e,2} Martin Hauer-Jensen^{b,2}

^a UAMS Myeloma Center, University of Arkansas for Medical Sciences, Little Rock, Arkansas 72205; ^b Division of Radiation Health, Department of Pharmaceutical Sciences, University of Arkansas for Medical Sciences, Little Rock, Arkansas 72205; ^c Department of Biochemistry and Molecular Biology, University of Arkansas for Medical Sciences, Little Rock, Arkansas 72205; ^d Division of Radioprotectants, Department of Pharmacology and Molecular Therapeutics, F. Edward Hébert School of Medicine, Uniformed Services University of the Health Sciences, Bethesda, Maryland 20814; ^e Armed Forces Radiobiology Research Institute, Uniformed Services University of the Health Sciences, Bethesda, Maryland 20814

Garg TK, Garg S, Miousse IR, Wise SY, Carpenter AD, Fatanmi OO, Rhee FV, Singh VK, Hauer-Jensen M. Modulation of Hematopoietic Injury by a Promising Radioprotector, Gamma-Tocotrienol, in Rhesus Macaques Exposed to Partial-Body Radiation. *Radiat Res.* 201, 55–70 (2024).

Currently, no radioprotectors have been approved to mitigate hematopoietic injury after exposure to ionizing radiation. Acute ionizing radiation results in damage to both hematopoietic and immune system cells. Pre-exposure prophylactic agents are needed for first responders and military personnel. In this study, the ability of gamma-tocotrienol (GT3), a promising radioprotector and antioxidant, to ameliorate partial-body radiation-induced damage to the hematopoietic compartment was evaluated in a non-human primate (NHP) model. A total of 15 rhesus NHPs were divided into two groups, and were administered either GT3 or vehicle 24 h prior to 4 or 5.8 Gy partial-body irradiation (PBI), with 5% bone marrow (BM) sparing. Each group consisted of four NHPs, apart from the vehicle-treated group exposed to 5.8 Gy, which had only three NHPs. BM samples were collected 8 days prior to irradiation in addition to 2, 7, 14, and 30 days postirradiation. To assess the clonogenic ability of hematopoietic stem and progenitor cells (HSPCs), colony forming unit (CFU) assays were performed, and lymphoid cells were immunophenotyped using flow cytometry. As a result of GT3 treatment, an increase in HSPC function was evident by an increased recovery of CFU-granulocyte macrophages (CFU-GM). Additionally, GT3 treatment was shown to increase the percentage of CD34⁺ cells, including T and NK-cell subsets. Our data further affirm GT3's role in hematopoietic recovery and suggest the need for its further development as a prophylactic radiation medical countermeasure. © 2024 by Radiation Research Society

¹ These authors contributed equally to this data.

² Corresponding authors: Vijay K. Singh, email: vijay.singh@usuhs.edu; Martin Hauer-Jensen, email: Mmhjensen@uams.edu.

INTRODUCTION

The risk of exposure to high doses of total- or partial-body ionizing radiation arising from accidental or intentional releases by terrorist attacks seems inevitable (1). Radiological/nuclear exposures may result in acute radiation syndrome (ARS) within a relatively short period, leading to hematopoietic (H-ARS), gastrointestinal (GI-ARS), or cutaneous and neurovascular injuries (2, 3). Two additional approved agents are biosimilars of Neulasta. Moreover, such exposures are more than likely to be non-uniform in nature and the severity of the injury depends on the dose absorbed, radiation quality, and the organ system that gets exposed (3). Among the various tissues and organs in the body, bone marrow (BM) is the most radiosensitive tissue. Damage to BM results in manifestations of ARS including myelosuppression, bleeding, immune dysfunction, systemic inflammation, and life-threatening infections secondary to BM failure (3, 4). Currently, the United States Food and Drug Administration (U.S. FDA) has approved only four medical countermeasures (MCMs) for H-ARS, and all are radiomitigators for use after radiation exposure (5–8). To date, there's no FDA-approved MCM that can be used prophylactically prior to radiation exposure for protection against unwanted/unexpected radiation injuries (9, 10). Hence, there is an urgent need to develop MCMs to protect against the devastating effects of radiation exposure that are safe, non-toxic, and effective, have excellent safety profiles, and can be easily stored, distributed, and administered.

The hematopoietic system is composed of both mature blood cells and hematopoietic stem cells (HSCs) in the BM compartment that are highly sensitive to radiation injury, and are crucial for the regeneration of blood cells (11). H-ARS mainly arises from hematopoietic insufficiency resulting in severe pancytopenia, which in turn increases life-threatening infections as well as vascular permeability and hemorrhage in

vital organs (12–15). In addition, due to the rapid proliferation rates and reduced DNA repair capacity of myeloid/lymphoid hematopoietic progenitors, the adverse effects caused by H-ARS may affect immune function and can potentially persist long-term (16–18). Therefore, protecting and rescuing HSCs and its self-renewable ability to repopulate hematopoietic progenitor cells (HPCs) is essential to mitigating H-ARS (11, 19, 20).

Over the past few decades, several natural products and their synthetic analogues have been found to be of interest for development as radiation MCMs, which exhibit injury-counteracting potential and minimal toxicity (21). Among them, members of the vitamin E family are well known for their anti-oxidative, anti-inflammatory, and neuroprotective properties (21–23). The vitamin E family comprises eight different isoforms: four saturated analogues called tocopherols (α , β , γ , δ) and four unsaturated analogues called tocotrienols (α , β , γ , δ), and are collectively referred as tocopherols (24, 25). These agents protect cells from increased oxidative damage caused by radiation-induced free radical generation (24, 25). GT3 has emerged as one of the most efficacious and promising radioprotectors tested to date. It is a natural antioxidant and a potent inhibitor of 3-hydroxy-3 methylglutaryl-coenzyme A (HMG-CoA) reductase (26–29). GT3 has been shown to improve mitochondrial respiration, coupling, and mitochondrial membrane potential, inhibit pro-apoptotic proteins and enhance anti-apoptotic proteins, inhibit NF- κ B activation, and reduce NF- κ B transcription activity (30). GT3 treatment has shown radioprotective efficacy in both rodents (mice) and NHPs when administered 24 h prior to total-body irradiation (TBI) (31, 32). Interestingly, the radioprotective effects of GT3 depend not only on its antioxidant properties, but also on its ability to accumulate in endothelial cells and reduce oxidative stress within epithelia and endothelia of various radiosensitive tissues (33). Though the mechanism of action of GT3 is not fully understood, the above attributes of GT3 may be contributing to preserve its antioxidant defense and avoid the pro-inflammatory response to prevent ionizing radiation-induced injury. Furthermore, GT3 has also been shown to enhance hematopoietic recovery in murine and NHP models (32, 34, 35). GT3 was found to stimulate an increase of HPCs in the BM of irradiated mice (35). In addition to HSCs and HPCs, GT3 reduced radiation-induced persistent DNA damage of lymphoid/myeloid progenitor cells, while significantly inducing G-CSF (granulocyte-colony stimulating factor), a crucial factor in stem cell mobilization and hematopoietic recovery (36, 37). Interestingly, GT3 also demonstrated its radioprotective role in intestinal epithelial and crypt cells in an NHP model exposed to a supra-lethal dose of radiation (38, 39). Most importantly, GT3 is under advanced development as a radioprotective MCM following the U.S. FDA Animal Rule to be used as a pre-exposure prophylaxis for H-ARS (31). Notably, in a recent study, we showed that GT3 accelerated recovery in CD34⁺ cells which increased HSC function as evidenced by improved

recovery of CFU-GM and burst-forming units-erythroid (BFU-E), and enhanced the recovery of circulating neutrophils and platelets in an NHP model of 4 and 5.8 Gy TBI (40).

The radioprotective efficacy of GT3 was investigated, as well as its ability to accelerate hematopoietic recovery in an NHP model exposed to 4 or 5.8 Gy partial-body X-rays with 5% BM sparing. There has been recent interest in studying the efficacy of MCMs using a PBI model, which allows for the understanding of the effects of MCMs on organ-specific injuries. The PBI model was developed to mimic a real-life radiation exposure scenario that would likely include sparing of some BM (41, 42). Although several studies have been performed in the PBI model to identify potential biomarkers and to support MCM development (43–45), this study is the first report, to the best of our knowledge that assesses the major immune cell populations in the BM of GT3-treated NHPs using the partial-body NHP exposure model with a linear accelerator (LINAC). In addition, we evaluated the prophylactic efficacy of GT3 in accelerating radiation-induced decreases in peripheral complete blood counts (CBC). Results from this study demonstrate that 4 or 5.8 Gy PBI significantly reduced various immune cells in the BM, including the self-renewable capacity of HPCs. Importantly, GT3 treatment accelerated HPCs function by improving the recovery of CFU-GM, in addition to enhancing the percentage of T- and NK-cell subsets. In brief, these data further affirm GT3's contribution to hematopoietic recovery and that this agent needs further investigation for its development as an MCM for prophylaxis.

MATERIALS AND METHODS

Experimental Design

The goal of this study was to use an NHP model to study hematopoietic injury resulting from partial-body X-ray irradiation and its recovery after administration of GT3. The 15 NHPs in this study were split into two groups: 8 animals were exposed to 4 Gy (sub-lethal) and the other 7 animals were exposed to 5.8 Gy (\sim LD_{20–30/60}). Within each radiation dose group, four animals were administered GT3 (37.5 mg/kg) and the other 4 animals were administered the vehicle. For the 5.8 Gy vehicle-treated group, there were only three animals (Table 1). Irradiation occurred 24 h after GT3 or vehicle administration.

Animals

Fifteen naïve rhesus NHPs (7 males and 8 females) were housed in an Association for the Assessment and Accreditation of Laboratory Animal Care (AAALAC)-International accredited facility. Prior to conducting the study, animals were quarantined for six weeks (46). Details regarding animal care, housing, health monitoring, and enrichment have been described in detail earlier (47, 48). The Guide for the Care and Use of Laboratory Animals was strictly adhered to throughout the study (49).

GT3 and Vehicle Administration

Either GT3 or the vehicle were injected subcutaneously (sc) at a dose of 37.5 mg/kg 24 h prior to irradiation. Callion Pharma (Jonesborough, TN) supplied GT3, which was used as an injectable formulation with a concentration of 50 mg/mL, as well as the vehicle, which was an olive oil formulation (50). The individual weight of each NHP decided the volume of drug or vehicle administered. The injection site preparation and drug/vehicle administration are discussed in detail earlier (51).

TABLE 1
Experimental Design for 15 NHPs Exposed to 4 and 5.8 Gy PBI

Hematopoietic Study (PBI, LINAC)							
NHP	Drug	Route	Dose (mg/kg)	Frequency	Irradiation Dose (Gy)	Age (years)	Body Weight Initial (kg)
4 (2F/2M)	GT3	sc	37.5	24 h prior to irradiation	4	3.80 ± 0.14	5.41 ± 0.37
4 (2F/2M)	Veh	sc	37.5	24 h prior to irradiation	4	3.60 ± 0.54	5.1 ± 0.75
4 (2F/2M)	GT3	sc	37.5	24 h prior to irradiation	5.8	3.35 ± 0.59	4.80 ± 0.47
3 (2F/1M)	Veh	sc	37.5	24 h prior to irradiation	5.8	3.60 ± 0.17	5.37 ± 0.19

Partial-Body Irradiation

The fasting, transportation, and sedation of the NHPs were similar to methods described earlier for TBI (52). For PBI, NHPs were irradiated one at a time using a 4 MV photon beam from an Elekta Infinity clinical LINAC. Anterior/posterior measurements of the NHPs at the location of the absorbed dose target ("core of the abdomen") were measured with a digital caliper. Irradiation procedures with LINAC, dose rate, and dosimetry have been described in detail earlier (53).

Each NHP was placed in the custom-built positioning device attached to the LINAC couch. The NHP's limbs were secured to the platform using restraints that were attached to the device. Animals were exposed to PBI with 5% bone marrow sparing. To achieve 5% bone marrow sparing, the irradiation field excluded the tibia, ankles, and feet of the animal. The field size of approximately 80 cm along its diagonal with a collimator angle of 45° was used to provide a field size that was large enough to fit the crown-to-knee of each NHP inside the field (crown-to-knee lengths of the NHPs varied 54–75 cm). The heart rate and temperature of NHPs were continuously monitored throughout the irradiation procedure (Advisor vital signs monitor, Smiths Medical, Dublin, OH). The specific desired dose was delivered, with a dose rate of approximately 1.3 Gy/min. To ensure a uniform radiation field, half of the absorbed dose was delivered with a beam along the anterior-posterior direction (gantry angle 0°), and the other half was delivered along the posterior-anterior direction (gantry angle 180°).

The calculation of the number of monitor units (MUs) required to deliver the requested absorbed dose was based on the dose rate to the abdominal core of the NHP. Each NHP was positioned supine on the platform with its coronal midline at 149 cm from the LINAC target. However, the dose rate to the abdominal core depends on the thickness of tissue that the beam must travel through from the surface to the core of the NHP. To account for the effect of variations in attenuation of the beam due to variations in the anterior-posterior (AP) separation of each NHP, the AP-separation of each NHP was measured prior to irradiation.

To determine absorbed dose rates to NHPs of various AP-separations, the absorbed dose rates to the center of a series of cylindrical water-filled polymethylmethacrylate NHP phantoms were measured using a Farmer ionization chamber (0.6-cc sensitive volume). Phantoms with diameters of 5.08, 6.99, 10.16, and 12.7 cm were used for these dose rate measurements. These phantom diameters covered the range of AP-separations of the NHPs that were experimentally irradiated (7–11 cm). The number of monitor units required to deliver the requested absorbed dose to the abdominal core was adjusted for the AP-separation of each individual NHP. The Farmer ionization chamber used for the dosimetry measurements in this study was calibrated at a National Institute of Standards and Technology (NIST)-traceable accredited dosimetry calibration laboratory. The calibration was in terms of absorbed dose-to-water. A water-to-soft tissue correction factor was applied to the dose rates determined by these irradiations. This ionization chamber-based dosimetry system is based on the calculation of the absorbed dose rate that is described in the American Association of Physicists in Medicine (AAPM) Task Group (TG)-51 protocol (54). The absorbed dose rates determined from ionization chamber measurements were used to determine a function of dose rate vs. phantom diameter (where phantom diameter corresponds to the AP-separation of the NHP). This empirical

function was then used to determine the dose rate to the abdominal core of each NHP (based on its individual AP-separation that was measured prior to irradiation). This function enables calculating the absorbed dose rate to the cores of NHPs that are intermediate in size between that of the phantoms in which the dosimetry measurements were performed.

BM Collection

Approximately 2 ml BM sample was collected 8 days prior to irradiation and on days 2, 7, 14, and 30 postirradiation. The site for BM collection was the iliac crest and the site was alternated between collection days. This procedure was conducted by trained study personnel as described earlier (40). For pain management, a single dose of buprenorphine ([0.005–0.03 mg/kg, intramuscularly (im) or sc] was administered. The BM sample was transferred to a sterile tube, and samples were then promptly shipped on wet ice via FEDEX priority overnight for analysis to the collaborator at the University of Arkansas for Medical Sciences. The cells were stained within 16 h and analyzed within 24–48 h.

Blood Collection and Complete Blood Counts (CBCs)

Blood was collected from NHPs at various time points during the study using either the cephalic or saphenous vein, and CBCs were analyzed with a Bayer Advia-120 cell counter as previously described (55, 56).

Bone Marrow CFU Assay

CFU assays were performed by culturing 1×10^5 BM cells collected on days -8, 2, 7, 14, and 30 using Methocult TM H4034 optimum (Stem Cell Technologies, Vancouver, Canada), as described recently (40). CFU-GM and burst-forming unit-erythroid (BFU-E) were scored on day 14.

Flow Cytometry and Gating Strategy

The detailed procedure for flow cytometry of BM cells and gating strategy is described in detail earlier (40). Briefly, RBC lysis was performed, and cell viability was assessed by the trypan blue dye exclusion method. In addition, we used eFlour 506, a fixable viability dye to exclude the dead cells during flow cytometric analysis. To establish a gating strategy and a compensation matrix, unirradiated NHP BM samples were used to run single stained controls, fluorescence minus one control, as well as a complete cocktail of all immune cell markers (40). A list of various fluorochrome-conjugated antibodies for specific antigens and details of the gating strategy used in this study is provided in Supplementary Table S1 and Supplementary Fig. S1³ (<https://doi.org/10.1667/RADE-23-00075.1.S1>), respectively.

³ Editor's note. The online version of this article (DOI: <https://doi.org/10.1667/RADE-23-00075.1>) contains supplementary information that is available to all authorized users.

Statistical Analysis

Various statistical analyses were performed using GraphPad Prism Version 9.1.0 (GraphPad Software, San Diego, CA). Two-way analysis of variance (ANOVA) tests were performed to determine the interaction between the GT3 and vehicle-treated groups across various time points. To compare the mean of each treatment group to the pre-irradiation time point (day -8), Dunnett multiple comparisons tests were performed. The student's t-test was also used to analyze pairwise comparisons. Statistical significance was set to a P value of 0.05 or less.

RESULTS

GT3 Effects on CBCs

A single dose of 37.5 mg/kg GT3-treatment 24 h prior to irradiation enhanced hematopoietic recovery in comparison to vehicle-treated NHPs as demonstrated in Figs. 1 and 2 and Supplementary Figs. S2 and S3 (<https://doi.org/10.1667/RADE-23-00075.1.S1>). Compared with the same dose of TBI, cytopenia and thrombocytopenia were less severe with PBI.

Effects of GT3 on CBC after 4 Gy PBI. GT3-treated NHPs exposed to 4 Gy PBI exhibited a higher level of WBC counts beginning at day 7 postirradiation (Fig. 1). GT3-treated NHPs showed higher neutrophil counts from day 7 and counts remained increased onwards. Reticulocytes in GT3-treated NHPs returned to pre-exposure levels by day 20, while vehicle-treated levels remained persistently high until day 30. The platelet levels in GT3-treated groups were not significantly altered compared to their respective vehicle-treated group. Unlike PBI, NHPs exposed to 4 Gy TBI showed pronounced reduction in the levels of neutrophils and platelets (40). This may be due to the lack of severe cytopenia with this dose of PBI compared with TBI. Further, both red blood cells (RBC) and hematocrit (HCT) showed an increased level on day 16 and 22 in GT3-treated groups. However, there was no significant difference between the groups at any other time points. Hemoglobin (HGB) showed a very similar pattern throughout the study with levels being slightly higher in GT3-treated groups. The GT3-treated NHPs showed higher levels of monocytes by day 20 and returned to baseline by day 30, while eosinophils showed increased levels by day 18 and remained elevated from day 26 to day 28 and returned to baseline by day 30. Lymphocytes and basophils followed very similar trends throughout the period of study (Supplementary Fig. S2; <https://doi.org/10.1667/RADE-23-00075.1.S1>).

Effects of GT3 on CBC after 5.8 Gy PBI. At 5.8 Gy, both GT3 and vehicle-treated groups exhibited very similar pattern in the levels of WBC, neutrophils and platelets after irradiation (Fig. 2). Notably, in comparison to 5.8 Gy PBI, NHPs with 5.8 Gy TBI showed a severe reduction in these parameters and recovery was found to be enhanced in GT3-treated groups (40). As stated above, this may be due to the lack of severe cytopenia with this dose of PBI. Reticulocyte levels were higher in GT3-treated groups on day 14, and in the following time points, both groups had very similar response patterns and reached baseline by day 30. Throughout the course of the

study, the response curve for RBCs, HGB and HCT levels in NHPs treated with GT3 closely resembled the response curve for those treated with the vehicle. Likewise, additional parameters like monocytes, lymphocytes and basophils showed little difference between GT3- and their respective vehicle-treated groups across the time points. The GT3-treated group showed an increased level of eosinophils from day 22 onwards and remained consistently higher than the control until day 30 ($P < 0.05$) (the latest time point examined in this study) (Supplementary Fig. S3; <https://doi.org/10.1667/RADE-23-00075.1.S1>).

GT3 Effects on BM Hematopoietic Injury

The effects of GT3 treatment on HSCs and immune cell phenotypes in BM samples were compared to their respective vehicle-treated group and to unirradiated animals on day 8 prior to PBI in each group. Figs. 3–10 illustrate these findings.

Leukocytes. The total number of white blood cell counts was based on the volume of aspirated BM. PBI revealed a progressive decrease in vehicle and GT3-treated groups until day 14 as shown in Table 2. Though these numbers returned to baseline by day 30 in the vehicle-treated group and close to baseline in the GT3-treated group at 4 Gy, these were relatively lower in both groups with 5.8 Gy (Table 2). These changes were significant on day 14 in the vehicle-treated group, and on day 2, 7 and 14 in the GT3-treated groups when compared with day -8 at 4 Gy. These changes were more prominent at 5.8 Gy on day 7 and 14 when compared to day -8 in the vehicle-treated group. At 5.8 Gy on day 30, the numbers were still lower in the vehicle-treated (51%) and GT3-treated group (35%) compared to day -8. However, these changes did not reach significance. In addition, no significant difference was observed between vehicle- and GT3-treated groups across the time points (Table 2).

Hematopoietic cells ($CD45^+$). A radiation dose of either 4 or 5.8 Gy PBI induced a decrease in hematopoietic cells in both vehicle- and GT3-treated groups (Fig. 3A and B). To prepare the BM cells for analysis, cells were labeled with CD45, a receptor linked protein tyrosine phosphatase present on most cells of the hematopoietic lineage (57). These changes were noted to be significant at day 2 in the vehicle-treated group (compared to day -8, $P < 0.001$) and at day 2 and 14 in the GT3-treated group at 4 Gy (compared to day -8, $P < 0.0001$, $P < 0.001$, respectively) (Fig. 3A). In addition, these changes were pronounced at 5.8 Gy in both groups on days 2, 7 and 14 compared to day -8 (Fig. 3B). A significant difference was also observed between the vehicle and GT3-treated groups on day 14 at 4 Gy ($P < 0.01$) (Fig. 3A).

Hematopoietic stem cells ($CD34^+CD45^+$). HSCs are the common precursors of immune cells and all blood lineages, and are crucial for maintaining the immune system (58). CD34 is a marker of HSCs in humans and NHPs (59, 60). Radiation doses of 4 and 5.8 Gy PBI induced a dose-dependent reduction in percent positive as well as in the total number of HSCs on days 2, 7 and 14 in both vehicle- and GT3-treated

CBC 4 Gy

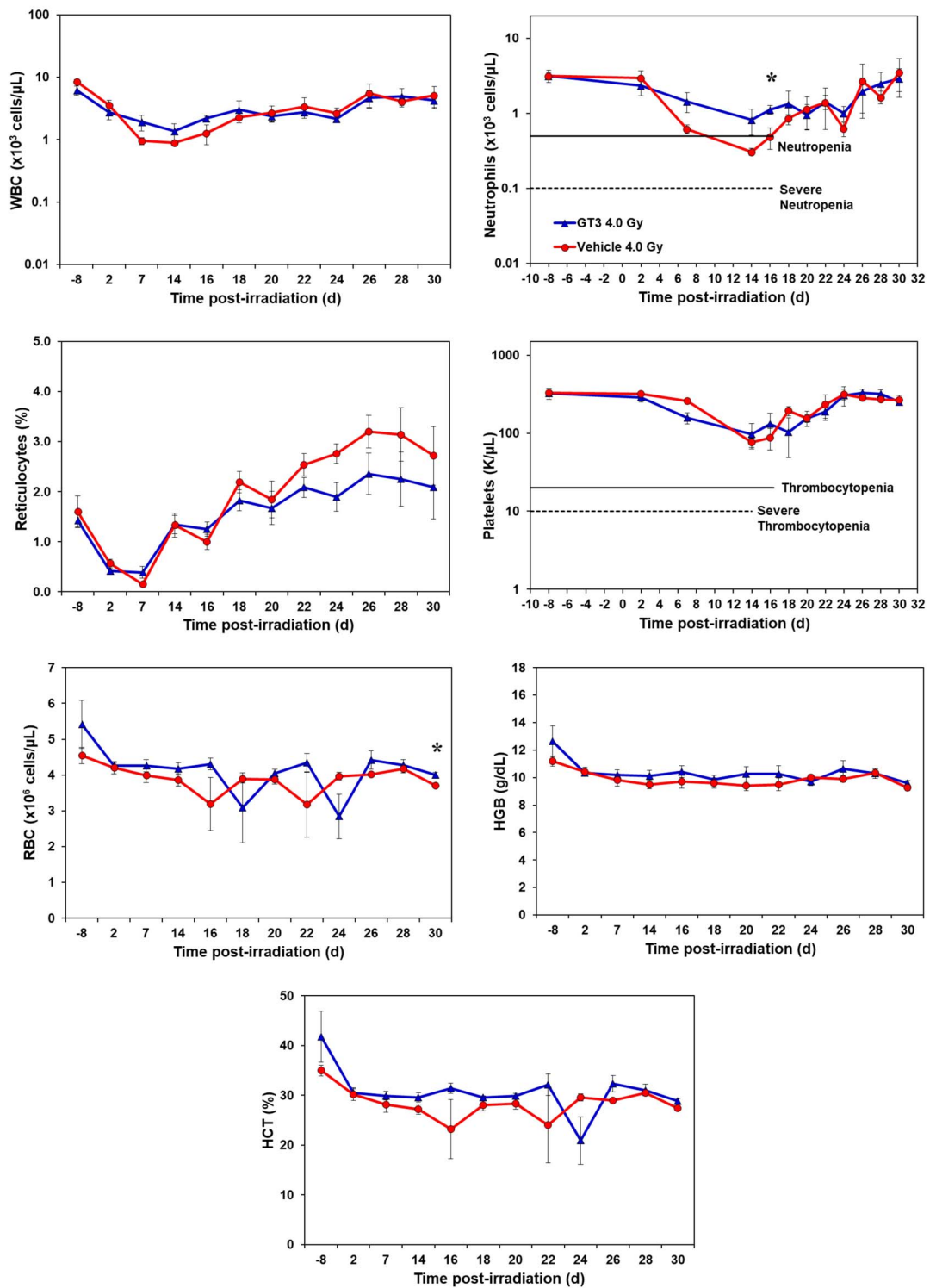


FIG. 1. CBC profiles in NHPs treated with a single dose of GT3 (37.5 mg/kg) or vehicle 24 h prior to 4 Gy PBI. Blood samples were collected at different time points as indicated in the graphs and cells were analyzed. Data are expressed as the mean \pm SEM. *A significant difference between the GT3- and vehicle-treated groups was determined when equal variance between groups was assumed (* $P < 0.05$).

CBC 5.8 Gy

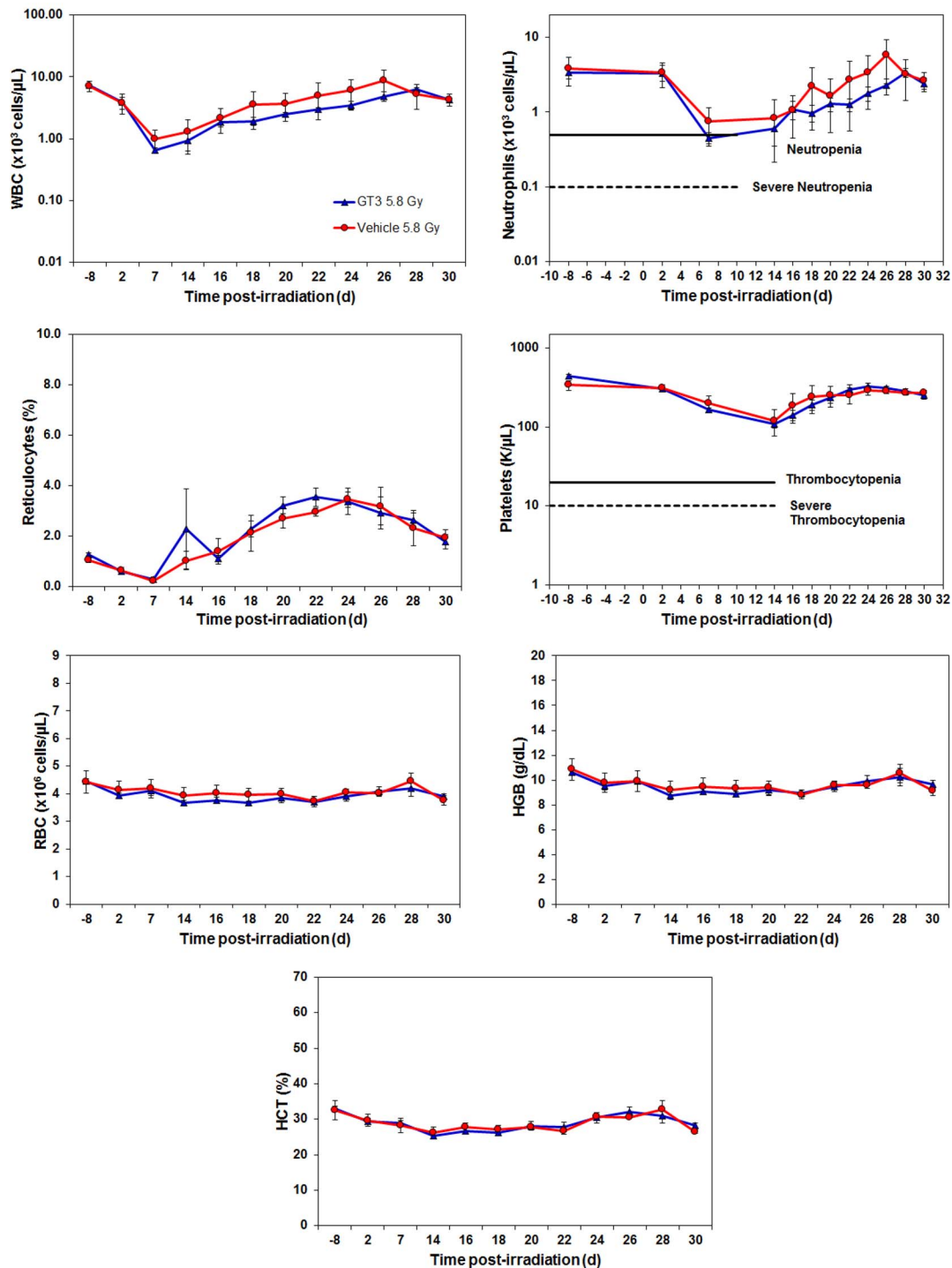


FIG. 2. CBC profiles in NHPs treated with a single dose of GT3 (37.5 mg/kg) or vehicle administered 24 h prior to 5.8 Gy PBI. Blood samples were collected at different time points as indicated in the graphs and cells were analyzed. Data are expressed as the mean \pm SEM.

groups as shown in Fig. 4 and Table 3. However, an apparent increase was observed in percentages on day 30, with significance in vehicle-treated groups at 4 and 5.8 Gy ($P < 0.05$) (Fig. 4C-D) and in the GT3-treated group at 5.8 Gy ($P < 0.001$) (Fig. 4D). A representative FACS plot has been shown for both 4 and 5.8 Gy PBI at day 30 (Fig. 4A-B).

Significant differences were also observed in the total number of these cells in GT3-treated groups on days 2, 7 and 14 at 4 Gy ($P < 0.01$) and on day 7 at 5.8 Gy ($P < 0.05$) (Table 3). However, in vehicle-treated groups, the total number appeared lower on days 2, 7, and 14 at 4 and 5.8 Gy, but these differences were not significant. Furthermore, the numbers

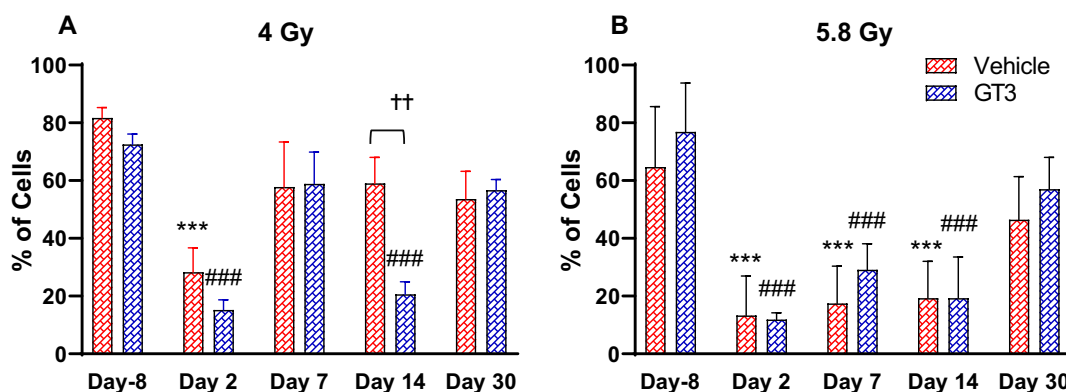


FIG. 3. Effects of GT3 on CD45⁺ expression in the BM of NHPs after irradiation. GT3 (37.5 mg/kg) or vehicle was administered to NHPs 24 h prior to 4 Gy (panel A) and 5.8 Gy (panel B) PBI. Data are expressed as the mean \pm SEM. *** $P < 0.001$ vs. vehicle day -8; ### $P < 0.001$ vs. GT3 day -8; †† $P < 0.01$ vehicle vs. GT3 at day 14.

and percent of HSCs were appreciably higher on day 30 in both vehicle- and GT3-treated groups at both doses of PBI (Fig. 4 and Table 3). The change in percentages of HSCs were in accordance with the total cell counts in BM.

B cells (CD3⁺CD20⁺). Radiation-induced reduction in the frequency of B cells were noted at all time points in vehicle-treated groups (19 to 66% decrease compared to day -8, $P < 0.05$, $P < 0.001$, $P < 0.01$) and in GT3-treated groups (decreased in the range of 39–86% compared to day -8, $P < 0.001$, $P < 0.01$) at 4 Gy (Fig. 5A). Populations of these cells declined further post 5.8 Gy PBI at all durations in GT3-treated groups (decreased in the range of 59 to 93% compared to day -8, $P < 0.05$, $P < 0.001$) (Fig. 5B). Though we observed a sharp decline in vehicle-treated groups at 5.8 Gy as well, these changes were not significant.

T cell (CD3⁺) subsets. T cells represent a major component of the adaptive immune system and play a critical role in cell-mediated immunity. Some of the major subsets of T cells have been immunophenotyped here and are discussed.

At 4 Gy after PBI, significant differences were noted in the frequency of T cells, T_H, and T_C subsets on day 2 compared to day -8 in both vehicle-treated and GT3-treated groups (Fig. 6A and B,D). In addition, a significant decrease was also recorded in T cells ($P < 0.01$), T_H cells ($P < 0.05$) and Treg cells ($P < 0.01$) in GT3-treated NHPs compared to their respective vehicle-treated NHPs on day 14 (Fig. 6A–D). This contrasts with what we observed at 4 Gy TBI, where no significant changes were noted in the frequencies of T cells,

T_H, Treg, and T_C subsets in vehicle- and GT3-treated groups across the time points. However, highly significant differences were observed on days 2, 7 and 14 in the frequencies of T cells and different T cell subsets in both vehicle- and GT3-treated groups at 5.8 Gy PBI (Fig. 6E and F,H). T cell percentage was decreased in the range of 59% to 81% in vehicle-treated groups and 56% to 77% in GT3-treated groups compared to day -8 (Fig. 6E). Similarly, T_H cell percentages were decreased in vehicle-treated groups in the range of 62% to 81% and in GT3-treated groups in the range of 40% to 86% (Fig. 6F). Likewise, T_C cells frequencies also declined sharply in vehicle-treated groups in the range of 62% to 83% and in the GT3-treated group in the range of 37% to 90% (Fig. 6H). On the contrary, we observed a general increase in the frequencies of T cells, T_H cells, and T_C cells on days 2, 7 and 14 in both vehicle- and GT3-treated groups exposed to 5.8 Gy TBI (40). Furthermore, no significant change was observed in Treg cells in either vehicle- or GT3-treated groups at 5.8 Gy PBI (Fig. 6G). A sharp, significant increase was observed in these cells at day 14 in vehicle-treated animals compared to the GT3-treated group at 4 Gy ($P < 0.01$) (Fig. 6C). Furthermore, we assessed the CD4:CD8 ratio, which indicates the overall immune health of an individual, and compared the values with the ratio at day -8 in both groups (4 and 5.8 Gy PBI). A significant increase was noticed in the ratio of these cells on day 2 in both vehicle- and GT3-treated groups after 4 Gy PBI (vehicle: 35%, $P < 0.01$; GT3: 27%, $P < 0.05$, respectively)

TABLE 2
Total Leukocytes in the BM of NHPs Exposed to 4 and 5.8 Gy PBI with and without GT3 Treatment

Days postirradiation	4 Gy		5.8 Gy	
	Vehicle	GT3	Vehicle	GT3
Day -8	25.87 \pm 2.22	33.39 \pm 12.88	39.57 \pm 19.14	32.8 \pm 9.92
Day 2	8.59 \pm 3.36	7.84 \pm 2.77	11.99 \pm 3.32	15.33 \pm 6.12
Day 7	2.41 \pm 0.77	5.53 \pm 2.15	2.72 \pm 1.26	1.34 \pm 0.19
Day 14	1.27 \pm 0.33	3.20 \pm 1.47	1.75 \pm 1.05	1.36 \pm 0.46
Day 30	25.59 \pm 13.95	19.85 \pm 7.18	19.25 \pm 10.22	21.45 \pm 5.94

Note. Absolute cell numbers [mean values \pm standard error (SEM)].

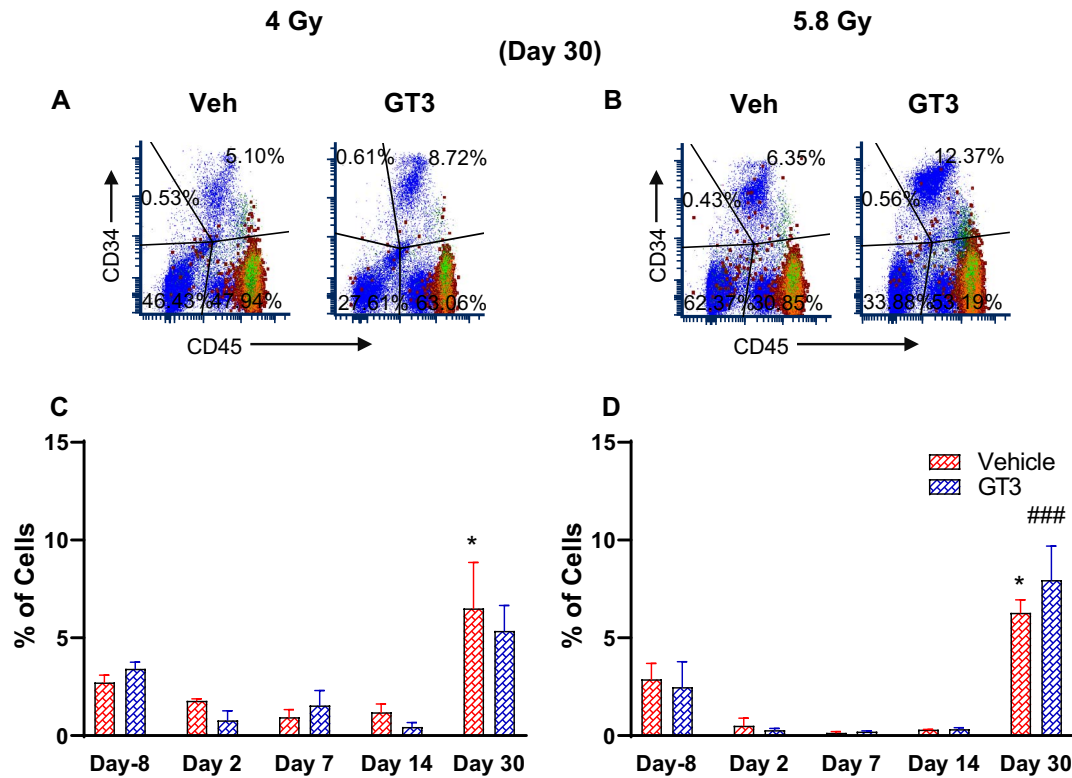


FIG. 4. Effects of GT3 on CD34 expression in the BM of NHPs after irradiation. GT3 (37.5 mg/kg) or vehicle was administered to NHPs 24 h prior to 4 Gy (panels A and C) and 5.8 Gy (panel B and D) PBI. The percentage of CD34⁺ cells (panels C and D) were analyzed in BM collected at different time points. Representative FACS plot on day 30 are shown after PBI (panels A and B). The number in each quadrant are the percentages based on the lymphocyte gate. Data are expressed as mean \pm SEM. *P < 0.05 vs. vehicle day -8; #P < 0.05, ###P < 0.001 vs. GT3 day -8.

(Fig. 7A), and in the GT3-treated group after 5.8 Gy PBI (40%, $P < 0.01$) (Fig. 7B).

NK cell subsets. A general time- and dose-dependent decrease was observed in the percentage of NK cells (CD3⁺CD56⁺) at 4 Gy and 5.8 Gy compared to baseline at day -8 in vehicle-treated animals after PBI (Fig. 8A and B). Nevertheless, these changes were not significant at any time point. However, in the GT3-treated group, a significant decrease was observed on day 2 and 14 at 4 Gy compared to day -8. (Fig. 8A). In contrast, in GT3-treated animals at 5.8 Gy, the percentage of NK cells appeared higher compared to the vehicle group at all durations, but significance was not achieved (Fig. 8B). The higher percentage of NK cells at 5.8 Gy may be attributed to GT3-mediated protection.

There was no significant difference observed in CD56⁺CD16⁺ (cytotoxic cells) subsets of NK cells at 5.8 Gy (Fig. 8D), apart from a significant decrease observed on day 14 in the GT3-treated group when compared to the respective vehicle-treated group ($P < 0.05$) at 4 Gy (Fig. 8C). A general decline was observed in the percentage of CD56⁺CD16⁻ expressing cells compared to day -8 in both vehicle- and GT3-treated groups on days 2, 14 and 30 at 4 Gy (Fig. 8E), and on days 2, 7 and 14 at 5.8 Gy (Fig. 8F). A significant difference was observed only on day 14 in the GT3-treated group (58% decrease, $P < 0.05$) (Fig. 8F). Though the percentage of these cells are on the lower side at different time points in the GT3-treated groups compared to day -8, these percentages are higher compared to their

TABLE 3
Total CD34⁺ Cells in the BM of NHPs Exposed to 4 and 5.8 Gy PBI with and without GT3 Treatment

Days postirradiation	4 Gy		5.8 Gy	
	Vehicle	GT3	Vehicle	GT3
Day -8	0.17311 \pm 0.0254	0.28220 \pm 0.1096	0.20667 \pm 0.0867	0.17500 \pm 0.1027
Day 2	0.01471 \pm 0.0029	0.00604 \pm 0.0035	0.00527 \pm 0.0039	0.00450 \pm 0.0017
Day 7	0.00227 \pm 0.0013	0.00578 \pm 0.0024	0.00035 \pm 0.0001	0.00048 \pm 0.0000
Day 14	0.00433 \pm 0.0023	0.00234 \pm 0.0013	0.00051 \pm 0.0001	0.00076 \pm 0.0002
Day 30	0.20619 \pm 0.1217	0.11061 \pm 0.0495	0.15015 \pm 0.0839	0.17939 \pm 0.0549

Note. Absolute cell numbers in millions [mean values \pm standard error (SEM)].

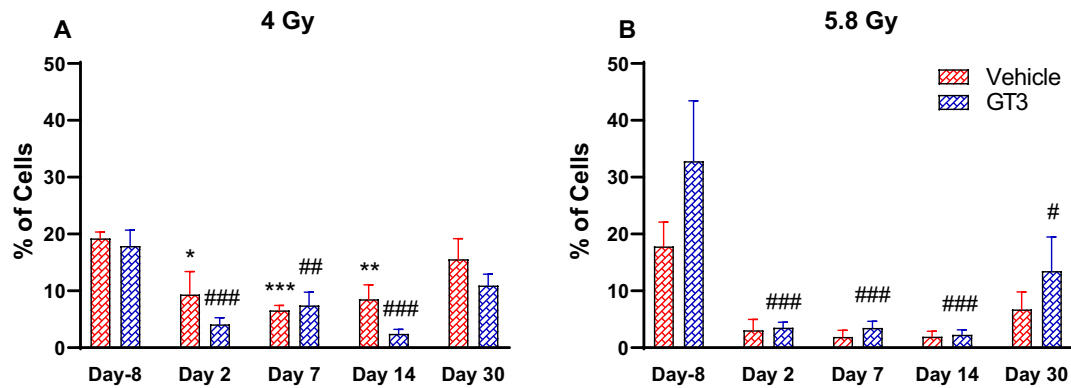


FIG. 5. Effects of GT3 on B⁺ cells in the BM of NHPs after irradiation. GT3 (37.5 mg/kg) or vehicle was administered to NHPs 24 h prior to 4 Gy (panel A) and 5.8 Gy (panel B) PBI. Data are expressed as the mean \pm SEM. *P < 0.05, **P < 0.01, ***P < 0.001 vs. vehicle day -8; #P < 0.05, ##P < 0.01, ###P < 0.001 vs. GT3 day -8.

respective vehicle-treated groups. Higher percentages of these cells in GT3-treated groups may be linked to GT3-mediated protection and regulation of other immune cells.

Monocytes and granulocytes (CD11b⁺). Granular leukocytes, or granulocytes, comprise of neutrophils, eosinophils and basophils, and serve as a key component in the innate immune system (57, 59). Although the percentage of granulocytes and monocytes appeared reduced in vehicle-treated animals on days 7 and 14 and in GT3-treated animals on days 2, 7, and 14 at 4 Gy, a significant difference was noticed only at day 14 in GT3-treated NHPs (>74% decrease compared to day -8, P < 0.01) (Fig. 9A). In addition, a progressive decrease in these cells was observed on days 2, 7, and 14 at the 5.8 Gy dose of PBI in both groups compared to day -8 (24 to 81% decrease in vehicle-treated and 19 to 68% decrease in GT3-treated (Fig. 9B). However, these cells returned to normal by day 30.

GT3 Effects on BM HPCs

To evaluate the effects of GT3 pre-treatment on HPCs, we performed in vitro clonogenic assays using BM cells from NHPs exposed to 4 and 5.8 Gy PBI. The number of CFUs serves as an indicator for hematopoiesis and is an important sign for hematopoietic recovery. We measured BM-CFUs in vehicle and GT3-treated groups at days -8, 2, 7, 14 and 30 after PBI. When compared to day -8, PBI significantly reduced the CFU-GM in both vehicle and GT3-treated groups at early time points: day 2 and day 7 in 4 Gy (Fig. 10A), and day 2 in 5.8 Gy (Fig. 10B). Importantly, when compared to their respective vehicle-treated groups, GT3-treated animals showed an increasing trend in CFU-GM from day 2 onwards, which persisted until day 30 in animals exposed to 4 and 5.8 Gy (Fig. 10A and B). This is consistent with what we observed in GT3-treated NHPs exposed to 4 and 5.8 Gy TBI, where GT3 improved the recovery of CFUs after irradiation (40). Interestingly, GT3 significantly increased CFU-GM levels by day 30 in GT3-treated groups when compared to its respective vehicle-treated groups in 4 Gy PBI, while 5.8 Gy dose of PBI

exhibited an increase in both vehicle- and GT3-treated groups (Fig. 10A-B). These data indicate that GT3 may enhance the ability of HPCs to differentiate into granulocytes and monocytes, and thereby may attenuate acute hematopoietic damage induced by radiation.

DISCUSSION

Radiation-induced hematopoietic injury and myelosuppression can occur in the event of a nuclear disaster, terror attacks or therapeutic interventions (3). HSC injury is one of the major causes of morbidity and mortality following exposure to a moderate or high dose of radiation (11, 13, 61). Studies have shown that even a sub-lethal dose of radiation can result in immunosuppression due to a decrease in the number of functional blood cells (62). Therefore, protecting and rescuing HSCs from radiation damage is not only critical for normal hematopoietic system function, but is also critical for the survival of cancer patients undergoing radiotherapy and for the development of MCMs (63–65). We have shown GT3 as a promising MCM with significant radioprotective efficacy both in mice and NHPs (31, 34, 39, 66, 67). GT3 is currently under advanced development for H-ARS (34). Most importantly, we recently showed an encouraging role of GT3 in promoting hematopoietic recovery in an NHP model with 4 or 5.8 Gy TBI by enhancing/preserving the self-renewable capacity of HSCs (40). Ultimately, the current study investigated GT3's potential in enhancing hematopoietic recovery in NHPs with 4 and 5.8 Gy PBI. Herein, we assessed radiation-induced changes in the immune cell phenotype in the BM treated with or without GT3 over a period of 30 days.

As stated above, studying PBI has benefits in the field of MCM development and radiation-induced injury progression. The hematopoietic system can recover better following high-dose irradiation if a small percentage of BM is spared. In this study, we used the PBI NHP model with 5% BM sparing to mimic radiation exposures that would likely spare some BM in a radiological/nuclear incidence. In such scenarios, radiation exposure may not be total-body and uniform. Moreover, several investigators in the field of MCM development have

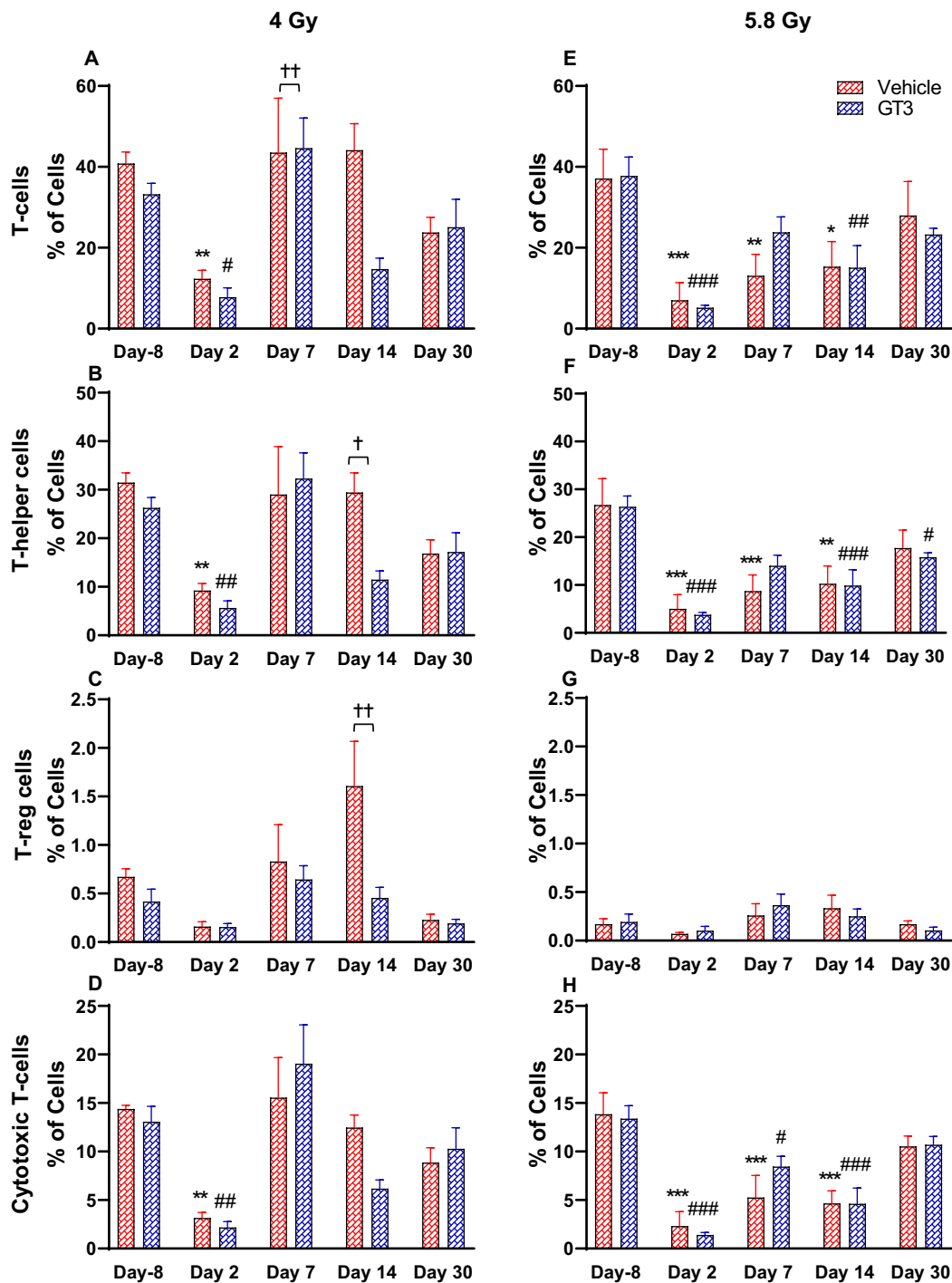


FIG. 6. Effects of GT3 on T cell marker expression in the BM of NHPs after irradiation. GT3 (37.5 mg/kg) or vehicle was administered to NHPs 24 h prior to 4 Gy and 5.8 Gy PBI. Expression of CD3⁺ cells (panels A and E), CD4⁺ cells (panels B and F), CD4⁺CD25⁺ cells (panels C and G), and CD8⁺ cells (panels D and H) were analyzed in BM collected at different time points. Data are expressed as mean \pm SEM. * $P < 0.05$, ** $P < 0.01$, *** $P < 0.001$. vs. vehicle day -8; # $P < 0.05$, ## $P < 0.01$, ### $P < 0.001$ vs. GT3 day -8; † $P < 0.05$ and †† $P < 0.01$ vehicle vs. GT3 at day 14.

emphasized the importance of this novel model to investigate the acute and delayed effects of radiation exposure and its usefulness for MCM efficacy (43, 68). NHPs have been shown to be an excellent model for studies of ARS and MCM development (69, 70). They closely resemble humans

with respect to their genetic homology, immune system and pathophysiology, and they are often used for the evaluation of immune system homeostasis and function, including for studies that assess MCM development (68–73). In addition, these animals show a reduction in circulating neutrophils

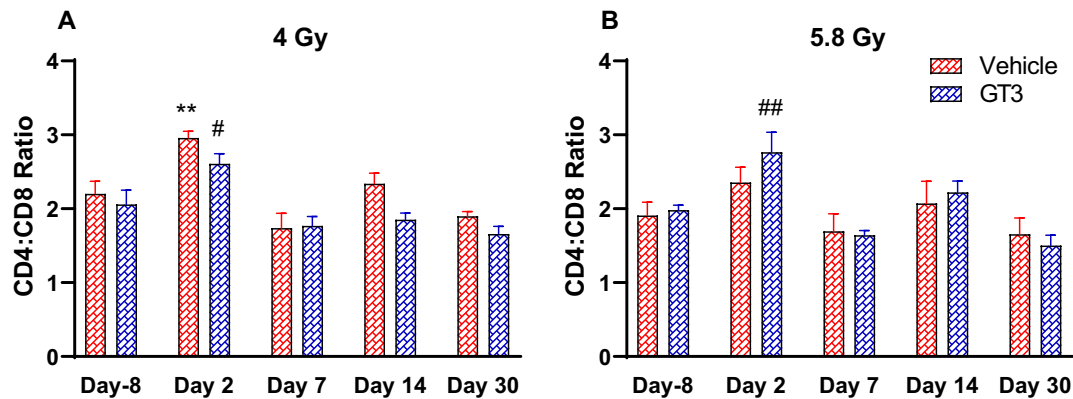


FIG. 7. Effects of GT3 on the CD4:CD8 ratio in the BM of NHPs after irradiation. GT3 (37.5 mg/kg) or vehicle was administered to NHPs 24 h prior to 4 Gy (panel A) and 5.8 Gy (panel B) PBI. Data are expressed as the mean \pm SEM. **P < 0.01 vs. vehicle day -8; #P < 0.05, ##P < 0.01 vs. GT3 day -8.

including a decrease in B cells, helper T cells (CD4⁺) and cytotoxic T cells (CD8⁺) associated with delays in T cell recovery following radiation, very much similar to humans (71, 74).

GT3, a potent antioxidant and a promising radioprotector (25, 31, 67), is under advanced development as a radioprotective prophylaxis MCM for H-ARS (34). Importantly, it has been observed that a single injection of GT3, compared to multiple doses of Neupogen/Leukine and two doses of Neulasta (with supportive care including blood products) was found to be equally effective (without supportive care/blood products) in ameliorating hematopoietic injury in an NHP model (31, 34, 67, 75, 76). Moreover, the radioprotective properties of GT3 relies not only on its free radical scavenging properties, but also on its ability to accumulate 30 – 50 times higher in endothelial cells. Notably, GT3 has been shown to protect endothelial cells from radiation-induced damage by enhancing the availability of nitric oxide synthase co-factor tetrahydrobiopterin (77). We have also shown that both GT3 and tetrahydrobiopterin supplementation reduce vascular peroxynitrite production following radiation (77). In addition, GT3 modulated irradiation-induced transcriptomic changes (53) and most importantly showed promising hematopoietic recovery in NHP models by stimulating/preserving the regenerating ability of the HSCs (34, 40). Here, we report that PBI doses of 4 and 5.8 Gy resulted in a marginal reduction in circulating neutrophils and platelets levels, including decreased reticulocytes. Notably, the severity and duration of neutropenia and thrombocytopenia with PBI were less compared with TBI at the same doses, 4 or 5.8 Gy (40). However, PBI induced a dose-dependent significant decrease in BM leukocyte populations including reduced percentages of HSCs and compromised HSC and HPC function. Interestingly, GT3 prophylaxis showed marginal efficacy in the recovery of HSCs and enhanced HPC function as revealed by increased CFUs with improved CBCs.

Radiation induces HSC damage and affects all lineages of blood cells, which are critical for producing and

maintaining blood cells in circulation (11, 78). Lymphocytes are shown to be highly sensitive to radiation (>2 Gy) and are the first to diminish from circulation followed by neutrophils and platelets. Moreover, radiation-induced depletion of cells in the peripheral blood (71) and bone marrow (79) may result in impaired immunity and subsequent infection later resulting in hemorrhages, which is a hallmark of H-ARS. The depletion and recovery of immune cells following radiation exposure requires HSC mobilization from the BM to reconstitute the hematopoietic system (68). Notably, GT3 has been shown to induce G-CSF and mobilize progenitors into circulation (36, 37). Interestingly, GT3-treated mice showed almost complete recovery of peripheral blood monocytes, neutrophils, and platelets by day 16 after TBI (32). Likewise, GT3 treatment reduced the severity and duration of neutropenia and thrombocytopenia in an NHP model with a radiation dose of 5.8 and 6.5 Gy TBI (34). Furthermore, we recently reported a similar observation, where GT3 was associated with improved recovery of WBCs, including neutrophils and platelets in irradiated NHPs (40). The current study is in concordance with our previous observation where GT3 treatment showed improved levels of WBCs, neutrophils, and reticulocytes following exposure to 4 and 5.8 Gy PBI. However, platelet levels were not altered much compared to the vehicle-treated irradiated controls. Importantly, PBI doses of 4.0 and 5.8 Gy did not induce significant hematopoietic injury and under such a situation, positive effects of GT3 are not obvious. Most importantly, this study clearly warrants a future study using a larger sample size, as we were limited with a small sample size of four animals per group and one group had only three NHPs. Keeping in mind this is a study with NHPs, these numbers were considered reasonable for a proof of principle study.

Exposure to radiation causes a drastic deficit in bone marrow populations. HSCs residing in the BM are characterized by their extensive self-renewal capacity and pluripotency. They give rise to the myeloid and lymphoid lineages and are responsible for maintaining the immune system (80). Several studies have extensively evaluated immune cell injury and

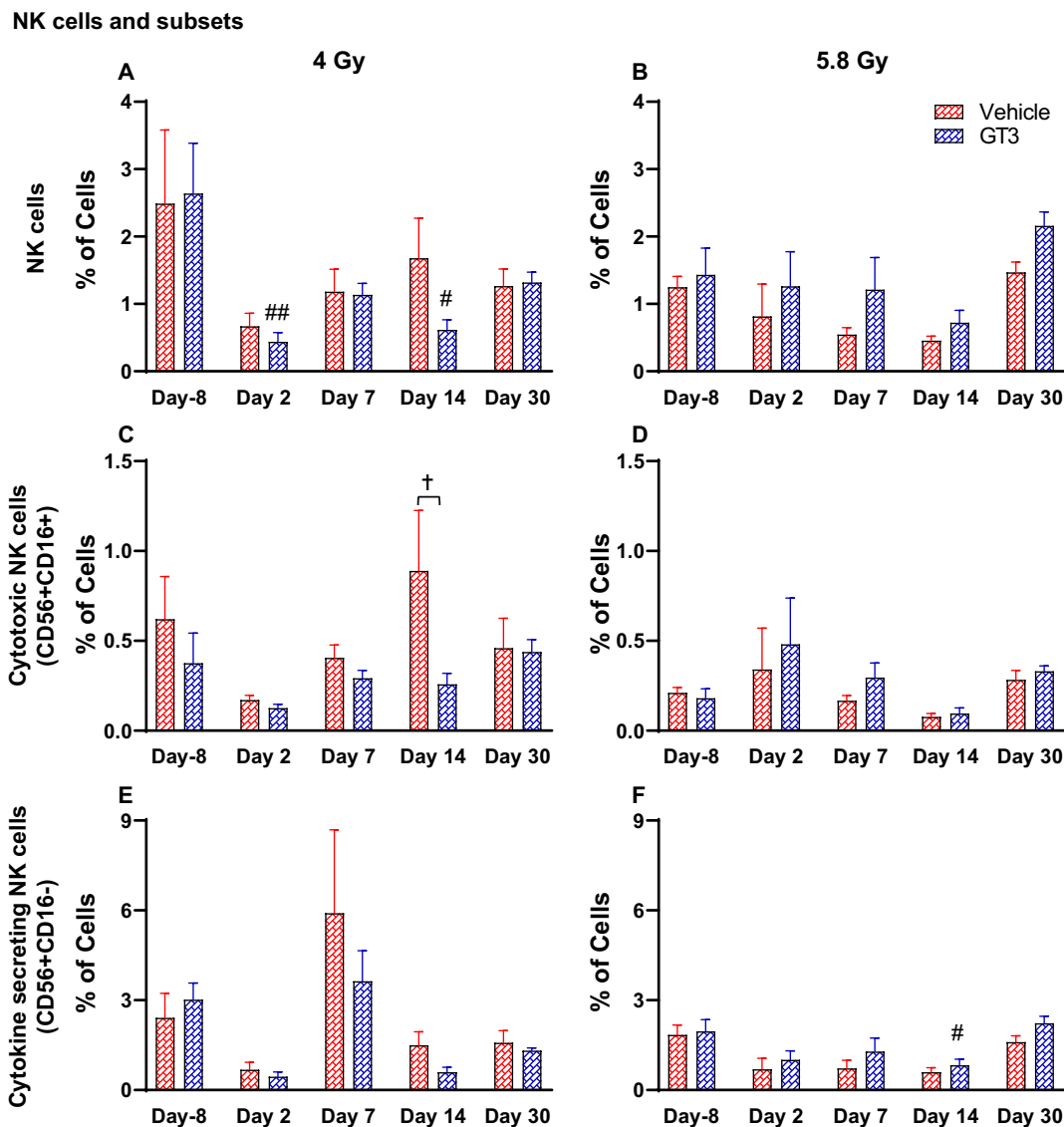


FIG. 8. Effects of GT3 on NK cell and subset expression in the BM of NHPs after irradiation. GT3 (37.5 mg/kg) or vehicle was administered to NHPs 24 h prior to PBI. Expression of CD56⁺ cells (panels A and B), CD56⁺CD16⁺ cells (panels C and D), and CD56⁺CD16⁻ cells (panels E and F) were analyzed in BM collected at different time points. Data are expressed as the mean \pm SEM. #*P* < 0.05, ##*P* < 0.01 vs. GT3 day -8; †*P* < 0.05, vehicle vs. GT3 at day 14.

recovery following high dose PBI with 5% BM sparing to a sub lethal TBI dose in NHP models (68, 70, 71, 74). Both models (TBI and PBI) have shown variable recovery kinetics of B- and T-cell populations in peripheral blood, suggesting their dependence on the marrow-derived stem and progenitor cells, peripheral homeostatic expansion and effective thymopoiesis (68, 71). Moreover, most of these studies have primarily assessed immune cell populations in the peripheral blood (B and/or T cells) with a few studies characterizing them in lymphoid organs (BM/spleen/thymus) (59, 60, 81, 82). Recently, our group showed that NHPs irradiated at a dose of 6.7 and 7.4 Gy TBI had significantly decreased total BM cells and CD45⁺ CD34⁺ HPSCs in the BM (60). Notably, irradiated cells have been shown to traffic to the BM and bring about the reduction of HSCs and HPCs (83). This is consistent with what we observed in

the current study, where PBI induced a dose-dependent decrease in different immune cells present in the BM, including HSCs and progenitors as reflected in their percentages. However, by day 30, HSC recovery was significantly increased in GT3- and vehicle-treated groups at both doses of PBI (latest time point examined in this study), suggesting sparing of BM might have contributed towards the recovery. In contrast, only the GT3-treated group showed the recovery of HSCs in NHPs exposed to 4 and 5.8 Gy TBI (40). Importantly, HSCs recovery is crucial for the adequate production of B cell progenitors as well as for HSC mobilization.

Radiation-induced hematopoietic toxicity manifesting as BM failure occurs mainly due to rapid depletion of the HPCs (11, 13, 62). The number of CFUs serve as both an indicator for hematopoiesis and an important sign of hematopoietic

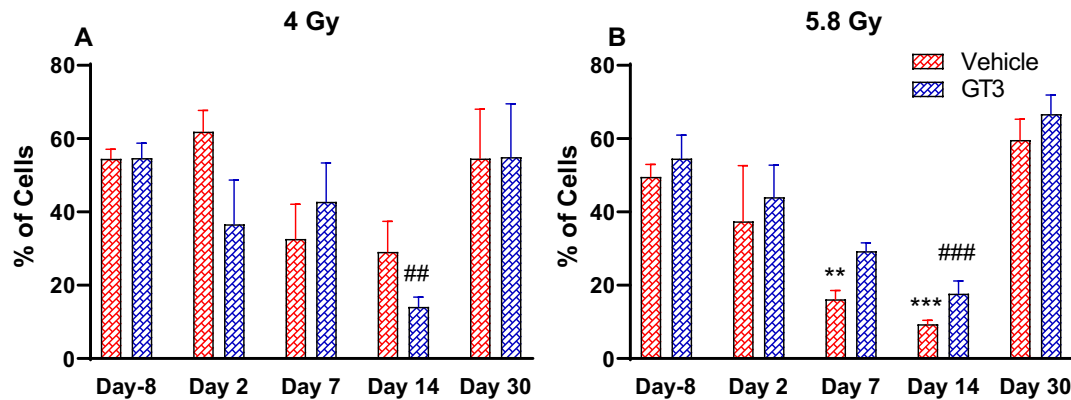


Fig. 9. Effects of GT3 on granulocyte and monocyte expression in the BM of NHPs after irradiation. GT3 (37.5 mg/kg) or vehicle was administered to NHPs 24 h prior to 4 Gy (panel A) and 5.8 Gy (panel B) PBI. Data are expressed as the mean \pm SEM. **P < 0.01, ***P < 0.01 vs. vehicle day -8; ##P < 0.01, ###P < 0.001 vs. GT3 day -8.

recovery (13, 84). Recently, we demonstrated that GT3 enhanced HPCs recovery by increasing the numbers of myeloid progenitors in the BM, like CFU-GM and BFU-E in an NHP model exposed to 4 and 5.8 Gy TBI (40). Likewise, in our current study, NHPs exposed to the same dose with PBI showed an accelerated recovery of CFU-GM in GT3-treated groups, noted as early as day 2, suggesting sparing of BM might have facilitated the recovery process. On the contrary, in our TBI study, we observed that GT3 treatment increased CFU-GM from day 7 onwards (40). Taken together, these results further confirm the earlier published studies in mice and NHPs that show GT3 is highly competent in protecting the hematopoietic tissue by facilitating/inducing HPCs recovery (34, 35, 40), and thereby promoting radiation-induced reduction in BM hematopoiesis.

Immune cells, including NK cells and T cells with different subsets such as CD3⁺, CD4⁺ and CD8⁺ cells, play an important role in maintaining immune function (85). The imbalance in the ratio of CD4⁺/CD8⁺ cells reflects the immunological status and serves as an important indicator of immune function in cancer patients (85). Studies have shown dynamic changes in the frequencies of these immune cell populations,

including their variable recovery kinetics in an NHP model after irradiation (68, 71, 74, 86). Further, in cancer patients, radiation-induced damage was associated with a decreased CD4/CD8 ratio, suggesting that the immune system was greatly compromised (85). In this study, we observed robust changes in the different subsets of T cells as a response to GT3. In GT3-treated groups, an increase in the number of CD4⁺ cells after PBI led to a shift in the ratio of CD4⁺/CD8⁺. This increase in the ratio may be associated with cytokine production, which might be imperative in the regulation of other immune cells in the BM microenvironment. This is consistent with what we observed in our earlier studies where the CD4/CD8 ratio was increased in GT3-treated groups after TBI (40). Further, in the B cell compartment, GT3-mediated protection from radiation-induced injury was observed only towards the end time point at 5.8 Gy PBI. Furthermore, NK cells, an important component of the innate immune system, are highly sensitive and this often results in their decreased number and activity as a reaction to radiotherapy (87). Here, we observed distinctive changes in the number of NK cells and their subsets after PBI in both vehicle- and GT3-treated groups. The higher number of NK cells and their subsets

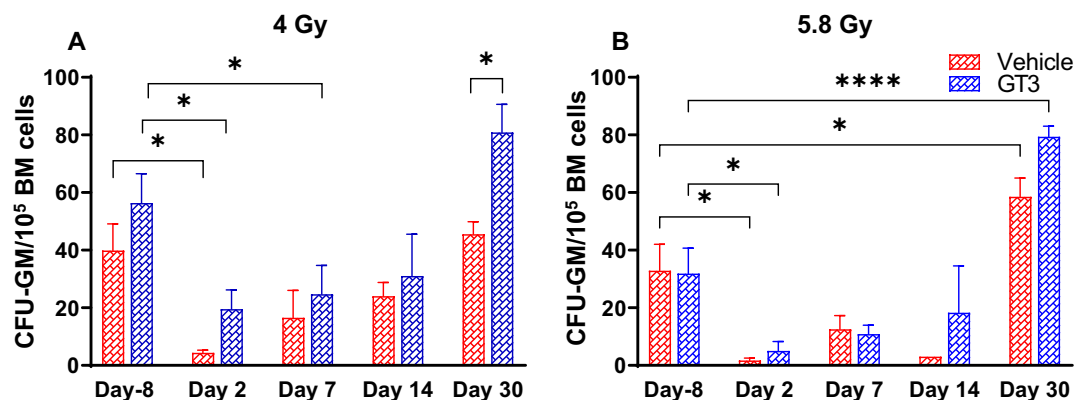


FIG. 10. Effects of GT3 on the BM-CFU_s post 14-day culture. Vehicle and GT3 (37.5 mg/kg) were administered to NHPs 24 h prior to 4 Gy (panel A) and 5.8 Gy (panel B) PBI. The clonogenic function of HSCs was analyzed in BM cells collected at different time points by CFU assay. Data are expressed as the mean \pm SEM. *P < 0.05, ****P < 0.0001.

observed in 5.8 Gy groups treated with GT3 can be attributed to GT3-mediated protection. This contrasts with what we observed in our TBI model, where GT3 treatment exhibited a significant reduction in NK cells and its subset (40). Notably, studies have shown NK cells to form synapses with their targets after irradiation, but then failed to undergo down-stream activation (88). Since mechanistic studies were beyond the scope of this study, it will be of great interest to assess the protective role of GT3 on irradiation-induced injury of NK cells.

To the best of our knowledge, this is the first study using the NHP partial-body irradiation model to investigate the potential of GT3 as a radioprotector for H-ARS. Taken together, the data in the current study points to the fact that GT3 has marginal efficacy when hematopoietic injury is minimal. We believe that this could be due to small sample size and low lethality of PBI at 4.0 and 5.8 Gy. This needs to be studied in the future with increased N and higher PBI doses of radiation to inflict significant hematopoietic injury with PBI.

SUPPLEMENTARY MATERIALS

Supplementary Fig. S1. Gating strategy for analyses of various immune cells in the NHP BM samples by flow cytometry.

Supplementary Fig. S2. Complete blood count (CBC) profiles in NHPs treated with GT3 or vehicle exposed to 4 Gy PBI. A single dose of GT3 (37.5 mg/kg) or vehicle was given to NHPs 24 h prior to irradiation. Peripheral blood samples were collected at different time points as indicated in the graphs and cells were analyzed with a Bayer Advia-120 cell counter. Data are expressed as the mean \pm SEM.

Supplementary Fig. S3. Complete blood count (CBC) profiles in NHPs treated with GT3 or vehicle exposed to 5.8 Gy PBI. A single dose of GT3 (37.5 mg/kg) or vehicle was given to NHPs 24 h prior to irradiation. Peripheral blood samples were collected at different time points as indicated in the graphs, and cells were analyzed with a Bayer Advia-120 cell counter. Data are expressed as the mean \pm SEM. *The difference between GT3- and vehicle-treated groups was significant when equal variance between groups was assumed (* $P < 0.05$).

Supplementary Table S1. Antibodies used for the analysis of NHP BM samples.

ACKNOWLEDGMENTS

The authors acknowledge the support from the Congressionally Directed Medical Research Programs (W81XWH-15-C-0117, JW140032) to VKS and sub-awarded to MH-J. We also acknowledge support by the National Institute of Health Center of Biological Research Excellence, grant P20GM109005, to MH-J. All animal procedures were approved by the BIOQUAL Institutional Animal Care and Use Committee (Protocol # 18-060) and the U.S. Department of Defense Animal Care and Use Review Office. All data relevant to this study are presented in the manuscript and supplementary files. The authors would like to thank the flow cytometry core at UAMS and BIOQUAL Inc., Rockville, MD. Authors declare no conflict of interest. The opinions or assertions contained herein are the

private views of the authors and are not necessarily those of the Uniformed Services University of the Health Sciences, or the Department of Defense.

Received: April 1, 2023; accepted: November 3, 2023; published online: December 7, 2023

REFERENCES

- Andersson KG, Mikkelsen T, Astrup P, Thykier-Nielsen S, Jacobsen LH, Schou-Jensen L, et al. Estimation of health hazards resulting from a radiological terrorist attack in a city. *Radiat Prot Dosimetry* 2008; 131:297-307.
- Andreyev HJ, Wotherspoon A, Denham JW, Hauer-Jensen M. "Pelvic radiation disease": new understanding and new solutions for a new disease in the era of cancer survivorship. *Scand J Gastroenterol* 2011; 46:389-97.
- Dorr H, Meineke V. Acute radiation syndrome caused by accidental radiation exposure - therapeutic principles. *BMC Med* 2011; 9:126.
- Koenig KL, Goans RE, Hatchett RJ, Mettler FA, Jr., Schumacher TA, Noji EK, et al. Medical treatment of radiological casualties: current concepts. *Ann Emerg Med* 2005; 45:643-52.
- Singh VK, Seed TM. An update on sargramostim for treatment of acute radiation syndrome. *Drugs Today (Barc)* 2018; 54:679-93.
- Singh VK, Seed TM. An update on romiplostim for treatment of acute radiation syndrome. *Drugs Today (Barc)* 2022; 58:133-45.
- Farese AM, MacVittie TJ. Filgrastim for the treatment of hematopoietic acute radiation syndrome. *Drugs Today (Barc)* 2015; 51:537-48.
- Singh VK, Seed TM. Radiation countermeasures for hematopoietic acute radiation syndrome: growth factors, cytokines and beyond. *Int J Radiat Biol* 2021; 97:1526-47.
- Singh VK, Seed TM. BIO 300: a promising radiation countermeasure under advanced development for acute radiation syndrome and the delayed effects of acute radiation exposure. *Expert Opin Investig Drugs* 2020; 29:429-41.
- Singh VK, Seed TM. Entolimod as a radiation countermeasure for acute radiation syndrome. *Drug Discov Today* 2021; 26:17-30.
- Shao L, Luo Y, Zhou D. Hematopoietic stem cell injury induced by ionizing radiation. *Antioxid Redox Signal* 2014; 20:1447-62.
- Singh VK, Newman VL, Seed TM. Colony-stimulating factors for the treatment of the hematopoietic component of the acute radiation syndrome (H-ARS): A review. *Cytokine* 2015; 71:22-37.
- Singh VK, Newman VL, Berg AN, MacVittie TJ. Animal models for acute radiation syndrome drug discovery. *Expert Opin Drug Discov* 2015; 10:497-517.
- Dainiak N. Hematologic consequences of exposure to ionizing radiation. *Experimental Hematology* 2002; 30:513-28.
- Wagemaker G. Heterogeneity of radiation sensitivity of hemopoietic stem cell subsets. *Stem Cells* 1995; 13 Suppl 1:257-60.
- Lumniczky K, Candeias SM, Gaipf US, Frey B. Editorial: Radiation and the immune system: Current knowledge and future perspectives. *Front Immunol* 2017; 8:1933.
- Heylmann D, Rödel F, Kindler T, Kaina B. Radiation sensitivity of human and murine peripheral blood lymphocytes, stem and progenitor cells. *Biochim Biophys Acta* 2014; 1846:121-9.
- So EY, Ouchi T. Decreased DNA repair activity in bone marrow due to low expression of DNA damage repair proteins. *Cancer Biol Ther* 2014; 15:906-10.
- Park E, Ahn G, Yun JS, Kim MJ, Bing SJ, Kim DS, et al. Dieckol rescues mice from lethal irradiation by accelerating hemopoiesis and curtailing immunosuppression. *Int J Radiat Biol* 2010; 86:848-59.
- Charrier S, Michaud A, Badaoui S, Giroux S, Ezan E, Sainteny F, et al. Inhibition of angiotensin I-converting enzyme induces radioprotection by preserving murine hematopoietic short-term reconstituting cells. *Blood* 2004; 104:978-85.

21. Singh VK, Beattie LA, Seed TM. Vitamin E: Tocopherols and tocotrienols as potential radiation countermeasures. *J Radiat Res* 2013; 54:973–88.
22. Sailo BL, Banik K, Padmavathi G, Javadi M, Bordoloi D, Kunnumakkara AB. Tocotrienols: The promising analogues of vitamin E for cancer therapeutics. *Pharmacol Res* 2018; 130:259-72.
23. Nesaretnam K. Multitargeted therapy of cancer by tocotrienols. *Cancer Letters* 2008; 269:388-95.
24. Palozza P, Simone R, Picci N, Buzzoni L, Ciliberti N, Natangelo A, et al. Design, synthesis, and antioxidant potency of novel alpha-tocopherol analogues in isolated membranes and intact cells. *Free Rad Biol Med* 2008; 44:1452-64.
25. Palozza P, Verdecchia S, Avanzi L, Vertuani S, Serini S, Iannone A, et al. Comparative antioxidant activity of tocotrienols and the novel chromanyl-polyisoprenyl molecule FeAox-6 in isolated membranes and intact cells. *Mol Cell Biochem* 2006; 287:21-32.
26. Pearce BC, Parker RA, Deason ME, Qureshi AA, Wright JJ. Hypocholesterolemic activity of synthetic and natural tocotrienols. *J Med Chem* 1992; 35:3595-606.
27. Qureshi AA, Pearce BC, Nor RM, Gapor A, Peterson DM, Elson CE. Dietary alpha-tocopherol attenuates the impact of gamma-tocotrienol on hepatic 3-hydroxy-3-methylglutaryl coenzyme A reductase activity in chickens. *Journal of Nutrition* 1996; 126:389-94.
28. Parker RA, Pearce BC, Clark RW, Gordon DA, Wright JJ. Tocotrienols regulate cholesterol production in mammalian cells by after transcriptional suppression of 3-hydroxy-3-methylglutaryl--coenzyme A reductase. *J Biol Chem* 1993; 268:11230–8.
29. Song BL, DeBose-Boyd RA. Insig-dependent ubiquitination and degradation of 3-hydroxy-3-methylglutaryl coenzyme a reductase stimulated by delta- and gamma-tocotrienols. *J Biol Chem* 2006; 281:25054-61.
30. Ding Y, Fan J, Fan Z, Zhang K. gamma-Tocotrienol reverses multidrug resistance of breast cancer cells through the regulation of the gamma-Tocotrienol-NF-kappaB-P-gp axis. *J Steroid Biochem Mol Biol* 2021; 209:105835.
31. Singh VK, Hauer-Jensen M. Gamma-tocotrienol as a promising countermeasure for acute radiation syndrome: Current status. *Int J Mol Sci* 2016; 17:e663.
32. Ghosh SP, Kulkarni S, Hieber K, Toles R, Romanyukha L, Kao TC, et al. Gamma-tocotrienol, a tocol antioxidant as a potent radioprotector. *Int J Radiat Biol* 2009; 85:598-606.
33. Naito Y, Shimozawa M, Kuroda M, Nakabe N, Manabe H, Katada K, et al. Tocotrienols reduce 25-hydroxycholesterol-induced monocyte-endothelial cell interaction by inhibiting the surface expression of adhesion molecules. *Atherosclerosis* 2005; 180:19-25.
34. Singh VK, Kulkarni S, Fatanmi OO, Wise SY, Newman VL, Romaine PL, et al. Radioprotective efficacy of gamma-tocotrienol in nonhuman primates. *Radiat Res* 2016; 185:285-98.
35. Kulkarni S, Ghosh SP, Satyamitra M, Mog S, Hieber K, Romanyukha L, et al. Gamma-tocotrienol protects hematopoietic stem and progenitor cells in mice after total-body irradiation. *Radiat Res* 2010; 173:738-47.
36. Singh VK, Wise SY, Fatanmi OO, Scott J, Romaine PL, Newman VL, et al. Progenitors mobilized by gamma-tocotrienol as an effective radiation countermeasure. *PLoS One* 2014; 9:e114078.
37. Kulkarni S, Singh PK, Ghosh SP, Posarac A, Singh VK. Granulocyte colony-stimulating factor antibody abrogates radioprotective efficacy of gamma-tocotrienol, a promising radiation countermeasure. *Cytokine* 2013; 62:278–85.
38. Garg S, Garg TK, Miousse IR, Wise SY, Fatanmi OO, Savenka AV, et al. Effects of gamma-tocotrienol on partial-body irradiation-induced intestinal injury in a nonhuman primate model. *Antioxidants (Basel)* 2022; 11:1895.
39. Garg S, Garg TK, Wise SY, Fatanmi OO, Miousse IR, Savenka AV, et al. Effects of gamma-tocotrienol on intestinal injury in a GI-specific acute radiation syndrome model in nonhuman primate. *Int J Mol Sci* 2022; 23:4643.
40. Garg TK, Garg S, Miousse IR, Wise SY, Carpenter AD, Fatanmi OO, et al. Gamma-tocotrienol modulates total-body irradiation-induced hematopoietic injury in a nonhuman primate model. *Int J Mol Sci* 2022; 23.
41. MacVittie TJ, Farese AM, Bennett A, Gelfond D, Shea-Donohue T, Tudor G, et al. The acute gastrointestinal subsyndrome of the acute radiation syndrome: a rhesus macaque model. *Health Phys* 2012; 103:411-26.
42. Shea-Donohue T, Fasano A, Zhao A, Notari L, Yan S, Sun R, et al. Mechanisms involved in the development of the chronic gastrointestinal syndrome in nonhuman primates after total-body irradiation with bone marrow shielding. *Radiat Res* 2016; 185:591-603.
43. MacVittie TJ, Bennett A, Booth C, Garofalo M, Tudor G, Ward A, et al. The prolonged gastrointestinal syndrome in rhesus macaques: the relationship between gastrointestinal, hematopoietic, and delayed multi-organ sequelae following acute, potentially lethal, partial-body irradiation. *Health Phys* 2012; 103:427-53.
44. Fish BL, MacVittie TJ, Gao F, Narayanan J, Gasperetti T, Scholler D, et al. Rat models of partial-body irradiation with bone marrow-sparing (leg-out PBI) designed for FDA approval of countermeasures for mitigation of acute and delayed injuries by radiation. *Health Phys* 2021; 121:419-33.
45. Jones JW, Bennett A, Carter CL, Tudor G, Hankey KG, Farese AM, et al. Citrulline as a biomarker in the non-human primate total- and partial-body irradiation models: Correlation of circulating citrulline to acute and prolonged gastrointestinal injury. *Health Phys* 2015; 109:440-51.
46. Phipps AJ, Bergmann JN, Albrecht MT, Singh VK, Homer MJ. Model for evaluating antimicrobial therapy to prevent life-threatening bacterial infections following exposure to a medically significant radiation dose. *Antimicrob Agents Chemother* 2022; 66:e0054622.
47. Singh VK, Fatanmi OO, Wise SY, Carpenter AD, Olsen CH. Determination of lethality curve for cobalt-60 gamma-radiation source in rhesus macaques using subject-based supportive care. *Radiat Res* 2022; 198:599-614.
48. Cheema AK, Li Y, Moulton J, Girgis M, Wise SY, Carpenter A, et al. Identification of novel biomarkers for acute radiation injury using multiomics approach and nonhuman primate model. *Int J Radiat Oncol Biol Phys* 2022; 114:310-20.
49. National Research Council of the National Academy of Sciences. Guide for the care and use of laboratory animals. 8th ed. Washington, DC: National Academies Press; 2011.
50. Pannkuk EL, Laiakis EC, Fornace AJ, Jr., Fatanmi OO, Singh VK. A metabolomic serum signature from nonhuman primates treated with a radiation countermeasure, gamma-tocotrienol, and exposed to ionizing radiation. *Health Phys* 2018; 115:3-11.
51. Cheema AK, Mehta KY, Fatanmi OO, Wise SY, Hinzman CP, Wolff J, et al. A Metabolomic and lipidomic serum signature from nonhuman primates administered with a promising radiation countermeasure, gamma-tocotrienol. *Int J Mol Sci* 2018; 19:79.
52. Cheema AK, Hinzman CP, Mehta KY, Hanlon BK, Garcia M, Fatanmi OO, et al. Plasma derived exosomal biomarkers of exposure to ionizing radiation in nonhuman primates. *Int J Mol Sci* 2018; 19:3427.
53. Vellichirammal NN, Sethi S, Pandey S, Singh J, Wise SY, Carpenter AD, et al. Lung transcriptome of nonhuman primates exposed to total- and partial-body irradiation. *Mol Ther Nucleic Acids* 2022; 29:584-98.
54. Almond PR, Biggs PJ, Coursey BM, Hanson WF, Huq MS, Nath R, et al. AAPM's TG-51 protocol for clinical reference dosimetry of high-energy photon and electron beams. *Med Phys* 1999; 26:1847-70.
55. Li Y, Singh J, Varghese R, Zhang Y, Fatanmi OO, Cheema AK, et al. Transcriptome of rhesus macaque (*Macaca mulatta*) exposed to total-body irradiation. *Sci Rep* 2021; 11:6295.
56. Carpenter AD, Li Y, Janocha BL, Wise SY, Fatanmi OO, Maniar M, et al. Analysis of the proteomic profile in serum of irradiated

- nonhuman primates treated with Ex-Rad, a radiation medical countermeasure. *J Proteome Res* 2023; 22:1116-26.
57. Radtke S, Adair JE, Giese MA, Chan YY, Norgaard ZK, Enstrom M, et al. A distinct hematopoietic stem cell population for rapid multilineage engraftment in nonhuman primates. *Sci Transl Med* 2017; 9.
 58. Wu G, Knabe DA, Flynn NE. Synthesis of citrulline from glutamine in pig enterocytes. *Biochem J* 1994; 299 (Pt 1):115-21.
 59. Zitsman JS, Alonso-Guallart P, Ovanez C, Kato Y, Rosen JF, Weiner JJ, et al. Distinctive leukocyte subpopulations according to organ type in cynomolgus macaques. *Comp Med* 2016; 66:308-23.
 60. Wang J, Shao L, Hendrickson HP, Liu L, Chang J, Luo Y, et al. Total body irradiation in the "hematopoietic" dose range induces substantial intestinal injury in non-human primates. *Radiat Res* 2015; 184:545-53.
 61. Wang Y, Schulte BA, LaRue AC, Ogawa M, Zhou D. Total body irradiation selectively induces murine hematopoietic stem cell senescence. *Blood* 2006; 107:358-66.
 62. Green DE, Rubin CT. Consequences of irradiation on bone and marrow phenotypes, and its relation to disruption of hematopoietic precursors. *Bone* 2014; 63:87-94.
 63. Singh VK, Seed TM. A review of radiation countermeasures focusing on injury-specific medicinals and regulatory approval status: part I. Radiation sub-syndromes, animal models and FDA-approved countermeasures. *Int J Radiat Biol* 2017; 93:851-69.
 64. Lopez M, Martin M. Medical management of the acute radiation syndrome. *Rep Pract Oncol Radiother* 2011; 16:138-46.
 65. Calvi LM, Frisch BJ, Kingsley PD, Koniski AD, Love TM, Williams JP, et al. Acute and late effects of combined internal and external radiation exposures on the hematopoietic system. *Int J Radiat Biol* 2019; 95:1447-61.
 66. Berbee M, Fu Q, Boerma M, Wang J, Kumar KS, Hauer-Jensen M. gamma-Tocotrienol ameliorates intestinal radiation injury and reduces vascular oxidative stress after total-body irradiation by an HMG-CoA reductase-dependent mechanism. *Radiat Res* 2009; 171:596-605.
 67. Singh VK, Seed TM. Development of gamma-tocotrienol as a radiation medical countermeasure for the acute radiation syndrome: Current status and future perspectives. *Expert Opin Investig Drugs* 2023; 32:25-35.
 68. MacVittie TJ, Bennett AW, M VC, Farese AM, Higgins A, Hankey KG. Immune cell reconstitution after exposure to potentially lethal doses of radiation in the nonhuman primate. *Health Phys* 2014; 106:84-96.
 69. Singh VK, Olabisi AO. Nonhuman primates as models for the discovery and development of radiation countermeasures. *Expert Opin Drug Discov* 2017; 12:695-709.
 70. MacVittie TJ, Farese AM, Jackson W, 3rd. The hematopoietic syndrome of the acute radiation syndrome in rhesus macaques: A systematic review of the lethal dose response relationship. *Health Phys* 2015; 109:342-66.
 71. Farese AM, Hankey KG, Cohen MV, MacVittie TJ. Lymphoid and myeloid recovery in rhesus macaques following total body X-irradiation. *Health Phys* 2015; 109:414-26.
 72. Thrall KD, Love R, O'Donnell KC, Farese AM, Manning R, MacVittie TJ. An interlaboratory validation of the radiation dose response relationship (DRR) for H-ARS in the rhesus macaque. *Health Phys* 2015; 109:502-10.
 73. Uno Y, Uehara S, Yamazaki H. Utility of non-human primates in drug development: Comparison of non-human primate and human drug-metabolizing cytochrome P450 enzymes. *Biochem Pharmacol* 2016; 121:1-7.
 74. Macintyre AN, French MJ, Sanders BR, Riebe KJ, Shterev ID, Wiehe K, et al. Long-term recovery of the adaptive immune system in rhesus macaques after total body irradiation. *Adv Radiat Oncol* 2021; 6:100677.
 75. Farese AM, Cohen MV, Katz BP, Smith CP, Gibbs A, Cohen DM, et al. Filgrastim improves survival in lethally irradiated non-human primates. *Radiat Res* 2013; 179:89-100.
 76. Hankey KG, Farese AM, Blaauw EC, Gibbs AM, Smith CP, Katz BP, et al. Pegfilgrastim improves survival of lethally irradiated nonhuman primates. *Radiat Res* 2015; 183:643-55.
 77. Berbee M, Fu Q, Boerma M, Pathak R, Zhou D, Kumar KS, et al. Reduction of radiation-induced vascular nitrosative stress by the vitamin E analog gamma-tocotrienol: evidence of a role for tetrahydrobiopterin. *Int J Radiat Oncol Biol Phys* 2011; 79:884-91.
 78. Venkateswaran K, Shrivastava A, Agrawala PK, Prasad A, Kalra N, Pandey PR, et al. Mitigation of radiation-induced hematopoietic injury by the polyphenolic acetate 7, 8-diacetoxy-4-methylthiocoumarin in mice. *Sci Rep* 2016; 6:37305.
 79. Till JE, McCulloch EA. A direct measurement of the radiation sensitivity of normal mouse bone marrow cells. *Radiat Res* 1961; 14:213-22.
 80. Wu AM, Till JE, Siminovitch L, McCulloch EA. Cytological evidence for a relationship between normal hematopoietic colony-forming cells and cells of the lymphoid system. *The Journal of experimental medicine* 1968; 127:455-64.
 81. Karlsson I, Malleret B, Brochard P, Delache B, Calvo J, Le Grand R, et al. Dynamics of T-cell responses and memory T cells during primary simian immunodeficiency virus infection in cynomolgus macaques. *J Virol* 2007; 81:13456-68.
 82. Spits H. Development of alphabeta T cells in the human thymus. *Nat Rev Immunol* 2002; 2:760-72.
 83. Kapoor V, Collins A, Griffith K, Ghosh S, Wong N, Wang X, et al. Radiation induces iatrogenic immunosuppression by indirectly affecting hematopoiesis in bone marrow. *Oncotarget* 2020; 11:1681-90.
 84. Park E, Ahn GN, Lee NH, Kim JM, Yun JS, Hyun JW, et al. Radioprotective properties of eckol against ionizing radiation in mice. *FEBS Letters* 2008; 582:925-30.
 85. Wang X-B, Wu D-J, Chen W-P, Liu J, Ju Y-J. Impact of radiotherapy on immunological parameters, levels of inflammatory factors, and clinical prognosis in patients with esophageal cancer. *J Radiat Res* 2019; 60:353-63.
 86. Hale LP, Rajam G, Carlone GM, Jiang C, Owzar K, Dugan G, et al. Late effects of total body irradiation on hematopoietic recovery and immune function in rhesus macaques. *PLoS One* 2019; 14:e0210663.
 87. Chen J, Liu X, Zeng Z, Li J, Luo Y, Sun W, et al. Immunomodulation of NK cells by ionizing radiation. *Front Oncol* 2020; 10:874.
 88. Zarcone D, Tilden AB, Lane VG, Grossi CE. Radiation sensitivity of resting and activated nonspecific cytotoxic cells of T lineage and NK lineage. *Blood* 1989; 73:1615-21.